Original Paper

Audiology & Neurotology

Audiol Neurotol 2012;17:290–298
DOI: 10.1159/000338406

Received: November 8, 2011
Accepted after revision: March 5, 2012
Published online: May 30, 2012

Cochlear Implant Insertion Forces in Microdissected Human Cochlea to Evaluate a Prototype Array

Yann Nguyen[a, c] Mathieu Miroir[a] Guillaume Kazmitcheff[a] Jasmine Sutter[a]
Morad Bensidhoum[b] Evelyne Ferrary[a, c] Olivier Sterkers[a, c]
Alexis Bozorg Grayeli[a, c]

[a]Inserm UMR-S 867, and [b]UMR CNRS 7052, Sorbonne Paris Cité, University Paris Diderot, Paris, and [c]Otorhinolaryngology Department, AP-HP, Beaujon Hospital, Clichy, France

Key Words
Cochlear implant · Inner ear trauma · Insertion force · Robotic surgery · Array insertion force

Abstract
Cochlear implant array insertion forces are potentially related to cochlear trauma. We compared these forces between a standard (Digisonic SP; Neurelec, Vallauris, France) and an array prototype (Neurelec) with a smaller diameter. The arrays were inserted by a mechatronic tool in 23 dissected human cochlea specimens exposing the basilar membrane. The array progression under the basilar membrane was filmed together with dynamic force measurements. Insertion force profiles and depth of insertion were compared. The recordings showed lower insertion forces beyond 270° of insertion and deeper insertions with the thin prototype array. This will potentially allow larger cochlear coverage with less trauma.

Introduction

Today, cochlear implantation is a routine technique for hearing rehabilitation [Wilson and Dorman, 2008]. Most implantees can achieve a speech recognition score for monosyllabic words of approximately 50–60% [Wilson and Dorman, 2008]. However, these performances are subject to a large interindividual variability. Factors influencing the outcome such as duration of deafness, age at implantation, duration of implantation, preexisting neurological diseases [Blamey et al., 1996], and preoperative speech performance [Gomaa et al., 2003] can rarely be improved. Nevertheless, speech performances after cochlear implantation have increased during the last 2 decades thanks to technical improvements. New speech-encoding strategies and optimized array designs were the most significant evolutions accounting for speech performances [Clark, 1996].

Emphasis has also been placed on minimizing the surgical trauma to the inner ear structures. The surgical technique has been modified to decrease the array-relat-

KARGER

Fax +41 61 306 12 34
E-Mail karger@karger.ch
www.karger.com

1420–3030/12/0175–0290$38.00/0

Accessible online at:
www.karger.com/aud

Alexis Bozorg Grayeli, MD, PhD
Otorhinolaryngology Department, Beaujon Hospital
100 Bd du Général Leclerc
FR–92118 Clichy Cedex (France)
Tel. +33 1 40 87 56 29, E-Mail alexis.bozorg-grayeli@bjn.aphp.fr

ed trauma [Lehnhardt, 1993]. The extension of cochlear implant indications to patients with residual hearing with the objective of preserving the residual hearing has boosted the research on minimally traumatic cochlear opening and array insertion [Kiefer et al., 2004]. Histological studies have shown that rigid arrays have a higher chance of perforating the basilar membrane and damaging the lateral wall. It has also been shown that straight arrays collide with the lateral wall at the end of the basal turn, and that thick arrays might rupture the basilar membrane in the cochlear apex by a radial pressure in the scala tympani [Eshraghi et al., 2003; Wardrop et al., 2005a, b]. These observations have led to the development of thinner, more flexible, and shorter arrays.

Several studies suggest that array insertion forces into the cochlea are related to cochlear trauma [Roland, 2005; Adunka and Kiefer, 2006]. Consequently, the assessment of these forces represents an interesting tool to evaluate the array's mechanical behavior and its design. Digisonic SP® (Neurelec, Vallauris, France) electrode arrays have been used for cochlear implantation since 2003 in a large population of cochlear implantees [Lazard et al., 2010]. In order to reduce the surgical trauma, a new prototype array with a smaller diameter, a softer silicone, and a modified disposition of the electrode contacts was designed. The goal of this study was to compare the insertion forces, the rate and location of basilar membrane rupture, the maximal inserted length, and the depth of insertion between the standard array (Digisonic SP) and the prototype array in a microdissected human cochlea model.

Materials and Methods

Human Temporal Bone Preparation

Twenty-nine fresh human temporal bones were prepared for array insertion. Each temporal bone was used for only 1 array insertion. In the first model, designated as microdissected cochlea (n = 23), the cochlea was dissected to expose an intact basilar membrane in its entire length (fig. 1). After resection of the bony auditory canal and middle ear cleft contents, the cochlea was exposed, and the bony otic capsule was thinned under microscope by diamond burrs at low speed. The scalae vestibuli and media were then carefully opened while respecting the basilar membrane integrity from the round window to the apex, and an extended round window opening was drilled using a 1-mm-diameter cutting burr. As the basilar membrane was previously exposed, the axis of the cochleostomy could be easily aligned with the center of the scala tympani at the basal turn. Before implantation, the basilar membrane was examined in detail for breach or displacement above its normal attachment under microscope. Only specimens with an intact basilar membrane were included.

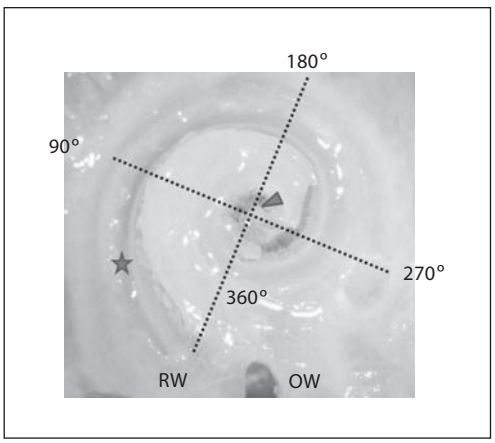

Fig. 1. Temporal bone preparation. Fresh human cochleae were harvested. The bony otic capsule was thinned using diamond burrs under microscopic vision. The scala vestibuli was then carefully opened while respecting the basilar membrane integrity, and an extended round window opening was drilled using a 1-mm-diameter cutting burr. The triangle represents the cochlea apex; the star represents the exposed basilar membrane along the first and second turn. RW = Round window; OW = oval window.

In the second model, designated as intact cochlea (n = 6), the cochlea and the round window region were exposed after bony external canal and middle ear cleft content removal. The bony otic capsule was left intact. Then, an extended round window opening was drilled in the same manner using a 1-mm-diameter cutting burr.

Specimens were placed individually in plastic boxes half filled with polyurethane resin (IPU 812; Trias Chem s.r.l., Parma, Italy) to allow fixing the anatomic specimen on a force sensor. Only the petrous apex was included in the resin and the insertion axis of the array was aligned to the z-axis of the force sensor. Resin spilling around the cochlea was carefully avoided.

Motorized Array Insertion Tool and Force Sensor

The insertion tool (fig. 2a) was composed of a rotary electrical motor (SPG30-300K®; Cytron Technologies, Skudai, Malaysia) mounted on a micromanipulator (Prior Scientific, Cambridge, UK). A threaded screw on the micromanipulator converted the rotation into a linear movement. Motor speed was controlled by the input voltage (range: 2.5–8.0 V) provided by an analog-to-digital interface card (Sensoray®, Tigard, Oreg., USA). The linear movement of the micromanipulator pushed the array by a blunt pin inside an insertion tube (fig. 2b).

Insertion forces were recorded with a 6-axis force sensor (ATI Nano 17®, calibration type SI-12-0.12, resolution 1/320 N; Apex, N.C., USA) (fig. 2c). Microdissected cochleae were fixed to the 6-axis force sensor. Data from the sensor were acquired at a sample rate of 100 Hz, recorded via an analog-to-digital interface card (Sensoray) and analyzed by in-house software. This program allowed the sensor recordings and the motor input voltage to be displayed in real time for synchronization with video recordings.

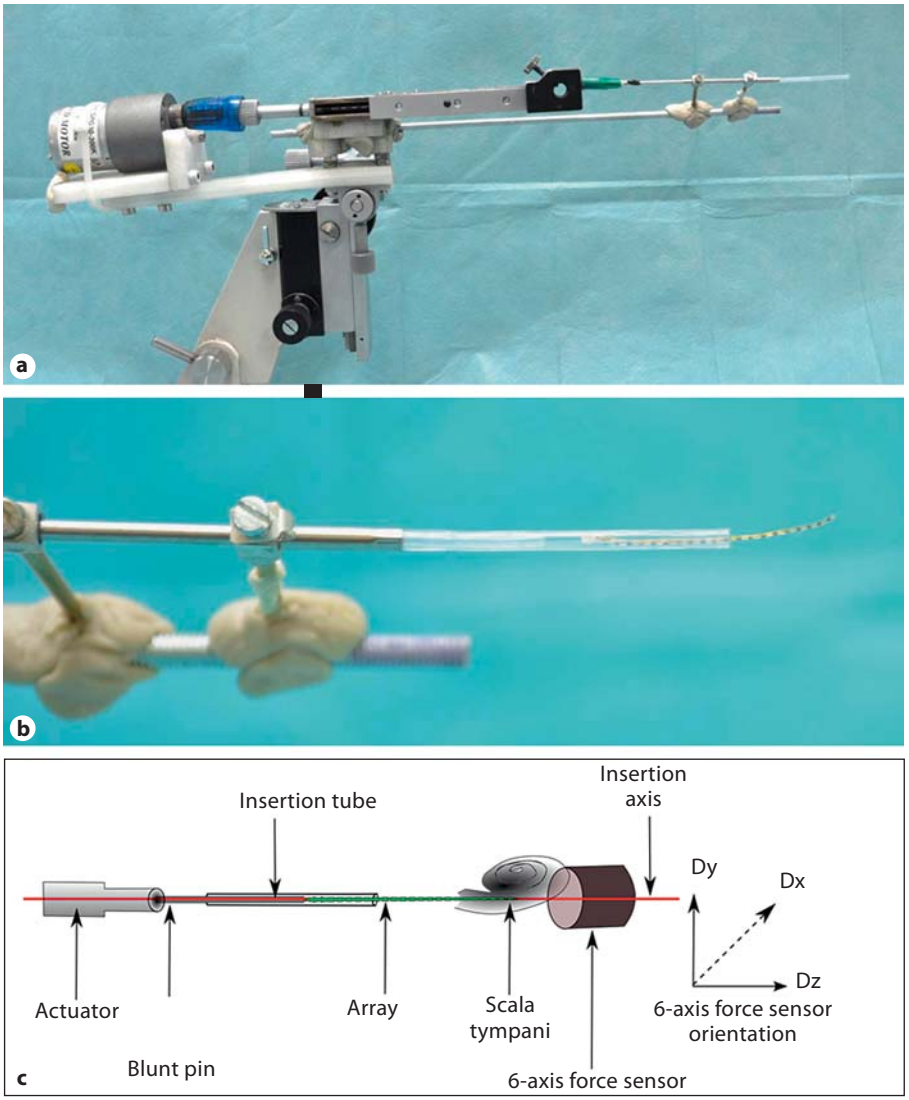

Fig. 2. The experimental setup. The in-house motorized insertion tool (**a**) was composed of a rotary motor mounted on a micromanipulator. A threaded screw on the micromanipulator converted the rotation to a linear actuation. The linear movement of the actuator pushed a blunt pin into an insertion tube and ejected the electrode array (**b**). Microdissected cochleae were molded into resin and fixed to a 6-axis force sensor which recorded the array insertion forces (**c**).

Electrode Arrays

Two electrode array designs were compared in this study.

The standard array (Digisonic SP; n = 8; fig. 3a) is composed of 20 electrodes, has a notched surface, a total length of 25 mm, a proximal diameter of 0.94 mm, a distal diameter of 0.5 mm, and a tapered distal tip diameter of 0.2 mm.

The prototype (n = 15; fig. 3b) also carried 20 electrodes and had a smooth surface, a total length of 24 mm, a proximal diameter of 0.5 mm, and a distal tip diameter of 0.4 mm (not tapered).

Array Insertions

The standard or prototype arrays were chosen randomly and were used only once for each experiment. Before array insertion, the force sensor was calibrated according to the manufacturer's procedure. The calibration was checked with a 1- and a 10-gram weight. The cochleae were filled with 0.9% saline. Hyaluronic acid gel (Healon®; AMO, Santa Ana, Calif., USA) was applied on the cochleostomy and in the insertion tube around the array. The insertion tool was aligned with the center of the scala tympani and placed adjacent to the cochleostomy without any contact with the bone to prevent interferences. Real-time high-definition video recording was performed with a reflex camera (Nikon D5000, Tokyo, Japan) connected to the operating microscope (Zeiss Universal OPMI1, Jena, Germany). The camera was aligned to the modiolus at 300 mm from the cochlea, and provided a perpendicular view of the entire basal turn at 11× magnification. Synchronization was insured by a sound signal on the film. The motor start could also be visualized on the real-time display via the voltage input recording. Insertion speed was set at 0.5 $mm \cdot s^{-1}$. The array insertion length was calculated based on the duration of insertion at the predefined speed.

Micro-CT Scanner

A Micro-CT scanner (Skyscan-1172®; Skyscan, Kontich, Belgium) was used on the 6 intact cochleae. The following settings were applied for acquisition: camera pixel size 9 μm, aluminum

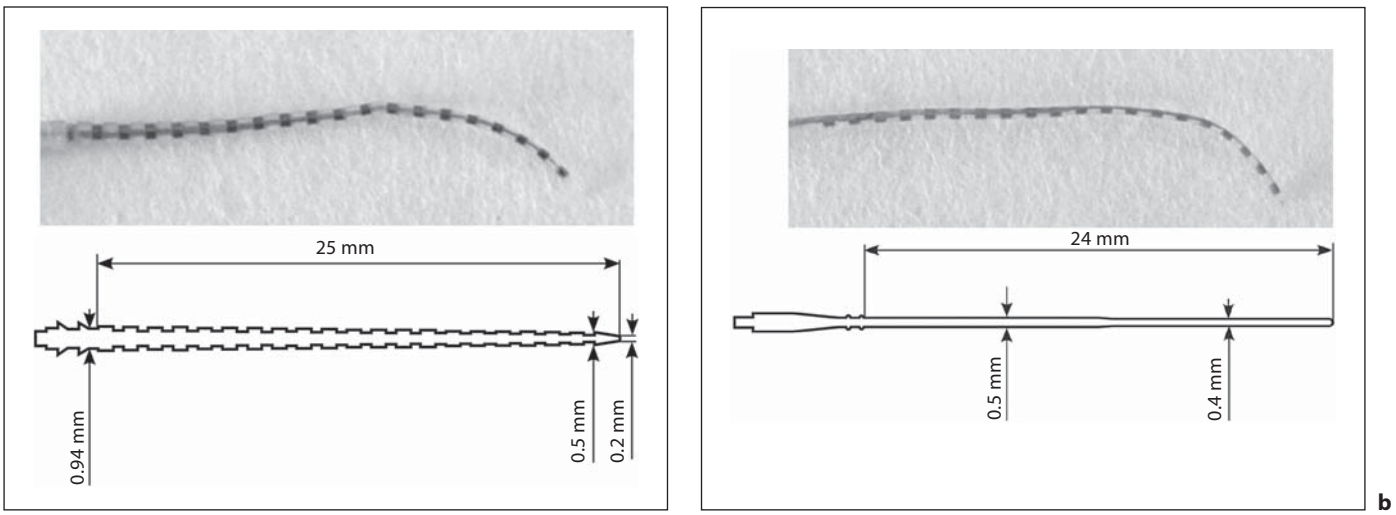

a b

Fig. 3. Standard (Digisonic SP) and prototype arrays. **a** The standard array is composed of 20 electrodes and has a notched surface. Dimensions: total length = 25 mm, proximal diameter = 0.94 mm, distal diameter = 0.5 mm, tapered distal tip diameter = 0.2 mm. **b** The prototype array also carried 20 electrodes but with a smooth surface. Dimensions: total length = 24 mm, proximal diameter = 0.5 mm, distal tip diameter = 0.4 mm.

filter, source voltage 80 kV, source current 100 μA. 3D reconstruction and curved multiplanar reconstruction were performed with NRecon® (Skyscan) and Osirix® (Kagi, Berkeley, Calif., USA). To evaluate the array position in the cochlea, a linear reconstruction along the array axis was performed. The array was considered in the scala tympani if it was visualized in the inferior half of the cochlear lumen in its whole length. The angle of insertion was measured and trauma to the osseous spiral lamina was also evaluated.

Data Analysis

After implantation, the temporal bones were carefully analyzed under the microscope and trauma was classified from grade 0 to 4 according to a cochlear trauma scale previously described [Eshraghi et al., 2003]. The insertion length and angle were measured on video recordings. The insertion force F was computed with the norm of the linear forces

$$F = \left(\sqrt{dx^2 + dy^2 + dz^2}\right).$$

Dynamic force profiles as well as maximal and mean insertion forces were collected. Data were analyzed using R (GNU software, http://www.cran.r-project.org/). A p value <0.05 was considered significant. Results are expressed as mean ± SD.

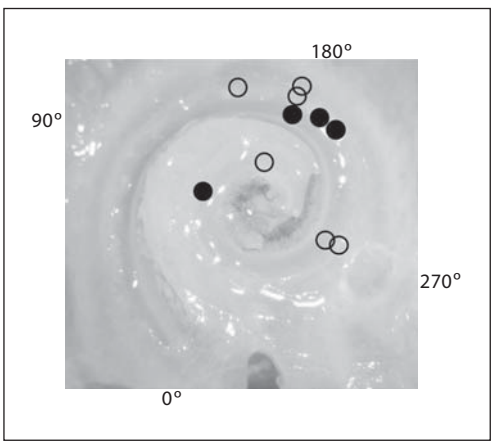

Fig. 4. Basilar membrane perforation sites in the microdissected cochlea model. Four of the 8 standard arrays (50%, ●) and 6 of the 15 prototype arrays (40%, ◯) perforated the basilar membrane.

Results

Microdissected Cochleae (n = 23)

Video Analysis

No folding array tip was observed on video analysis. Four of the 8 standard arrays (50%) and 6 of the 15 prototype arrays (40%) perforated the basilar membrane (fig. 4). The majority of the perforation sites were close to 180° (60%), suggesting that this region is critical during array progression. Trauma assessment according to the Eshraghi classification yielded 2 grade 0, 2 grade 1, and 4 grade 3 in the standard array group, and 5 grade 0, 4 grade 1, and 6 grade 3 in the prototype array group. The depth of insertion was highly correlated to the insertion length (y =

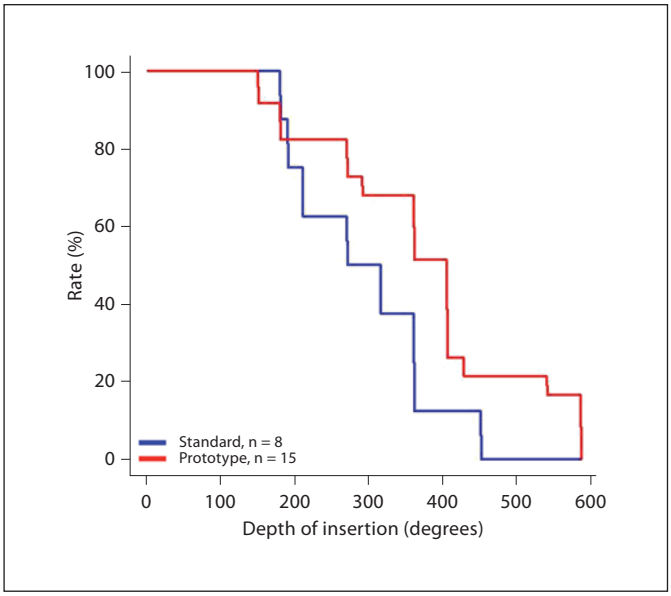

Fig. 5. Rate of array progression as a function of insertion depth. Prototype arrays were inserted significantly deeper than standard arrays without basilar membrane perforation (log-rank test, $p < 0.01$).

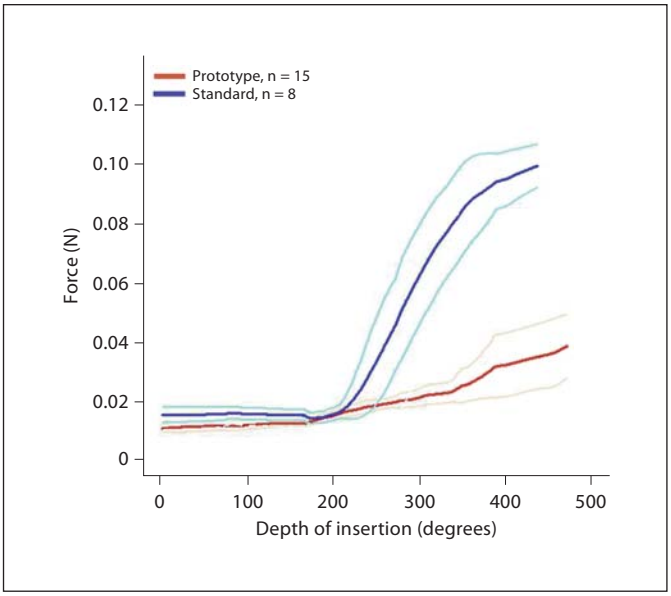

Fig. 6. Dynamic insertion force profiles as a function of insertion depth. Insertion forces were compared between standard and prototype arrays in their whole length in microdissected cochleae. Dynamic recordings in the prototype group showed significantly lower insertion forces in comparison to the standard group (from 0° to 540°, repeated-measures ANOVA, $p < 0.01$).

20.5x – 76.7, y = insertion depth in degrees, x = insertion length in millimeters, $R = 0.9$, $p < 0.0001$, ANOVA, $n = 23$). The mean insertion length without basilar membrane perforation was similar in the prototype and standard groups (21 ± 6.2 mm, n = 15 vs. 18 ± 4.2 mm, n = 8, respectively, not significant, unpaired t test). Similarly, the mean depth of insertion without basilar membrane perforation was similar in both groups (270 ± 140°, n = 15 vs. 202 ± 96° n = 8, respectively, not significant, unpaired t test). However, a Kaplan-Meier analysis showed that a deeper insertion without basilar membrane perforation could be obtained in the prototype group compared to the standard array group (log-rank test, $p < 0.01$; fig. 5).

Force Sensor Measurements

The mean insertion forces were similar in the standard and the prototype groups (0.03 ± 0.064 N, n = 8 vs. 0.01 ± 0.012 N, n = 15, respectively, not significant, unpaired t test). However, dynamic recordings showed significantly lower insertion forces in the prototype group in comparison to the standard arrays (repeated-measures ANOVA, $p < 0.01$; fig. 6). During the first half of the insertion (<200°) the insertion forces were very low for both arrays (<0.02 N). In the second part of the insertion, the force increased linearly for the standard array reaching 0.1 N while it remained below 0.05 N for the prototype array. A 32% reduction of overall friction forces was observed in the prototype group versus the standard group. It is noteworthy that basilar membrane perforations could not be detected on real-time force recordings (fig. 7).

Intact Cochlea (n = 6)

Three standard and 3 prototype arrays were implanted in 6 intact cochleae. One of the 3 standard arrays could only be partially inserted. One of the 3 prototype arrays had a folding tip after insertion.

Postimplantation Imaging

Four arrays (2 prototypes and 2 standard arrays) were fully inserted and positioned laterally in the scala tympani (fig. 7, 8a). The CT scan confirmed the partial insertion of 1 standard array (15 mm; fig. 8b) and detected a folding tip in 1 prototype array (fig. 8c). A curved multiplanar reconstruction of the cochlear lumen along the array showed that these arrays were placed in the inferior half of the cochlear lumen corresponding to the scala tympani in their whole length (fig. 8). The insertion depth for the fully inserted prototype arrays was 360° and 450°.

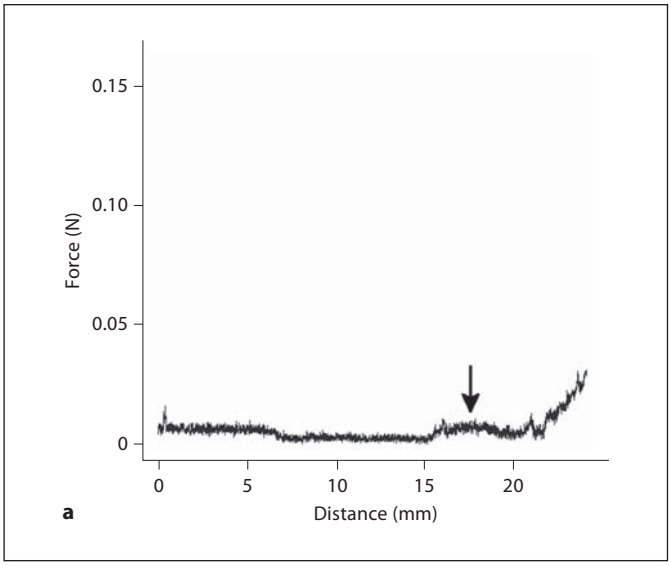

Fig. 7. Insertion force profile in a traumatic insertion. The video recording was synchronized with the insertion force measurement. **a** The perforation of the basilar membrane could be identified on the video recording. **b** No event could be detected on the force recordings at the moment of basilar membrane perforation. The insertion length at the perforation site is represented by the black arrow.

For the standard arrays this depth was 260° and 360°. No fracture of the bony lamina spiralis was detected on the imaging. Examination under microscope after microdissection revealed a grade 0 trauma (Eshraghi classification) in all 4 implanted samples with full insertion. Data concerning trauma in the cochleae with folding array tip and partial insertion were not available.

Force Sensor Measurements

Mean insertion forces in intact cochlea were similar to those in microdissected cochleae for fully inserted arrays: 0.03 and 0.02 N for the 2 prototype arrays, 0.05 and 0.04 N for the 2 standard arrays.

The mean insertion forces were higher in the partially inserted standard array (0.2 N; fig. 9b) and in the prototype array with a folding tip (0.10 N; fig. 9c) in comparison to the fully inserted arrays (fig. 9a). Moreover, the peak exceeded 0.3 N in the case of partial insertion or folding tip while it remained below 0.15 N in fully inserted arrays. Finally, the rising segment of the curve began earlier in the case of insertion abnormality (at 7 mm for the folding tip array and 10 mm for the partially inserted array) in comparison to fully inserted arrays (20 mm).

Discussion

Our model of microdissected cochlea combines a dynamic visualization of the cochlear implant array progression in human temporal bones and insertion force measurements. Minimizing the inner trauma and obtaining deeper array insertions are the objectives of the cochlear implantation with hearing preservation. Hence, the passive mechanical properties of the arrays are now considered as important as the electrical components of the cochlear implants. Our model offers the possibility to evaluate array designs with enhanced possibilities compared to the previously reported methods of array evaluation.

Originality of Our Insertion Force Measurement Model

Several studies have previously described models of array friction force measurements [Roland, 2005; Adunka and Kiefer, 2006; Radeloff et al., 2009]. The majority of experimental protocols employed artificial scala tympani models [Adunka and Kiefer, 2006; Radeloff et al., 2009; Majdani et al., 2010], and only one study reported friction force in anatomic specimens [Roland, 2005]. Transparent acrylic models of scala tympani at a 1/1 scale allow a visual control of the array progression and can be used repeatedly without any structural modifications. Therefore, they represent an adapted model for in vitro array comparison. However, friction forces measured in acrylic models differ from those measured in temporal bones. Roland [2005] observed that forces in formalin-fixed temporal bones could be twice as high as those recorded in an epoxy model using the same array and force sensor. It is reasonable to presume that the difference between the coefficient of friction of the endosteal lining and the lubricated acrylic with the array account for the observed difference. Furthermore, histological study coupled to insertion forces can only be performed in temporal bones. A rupture of the basilar membrane, an array

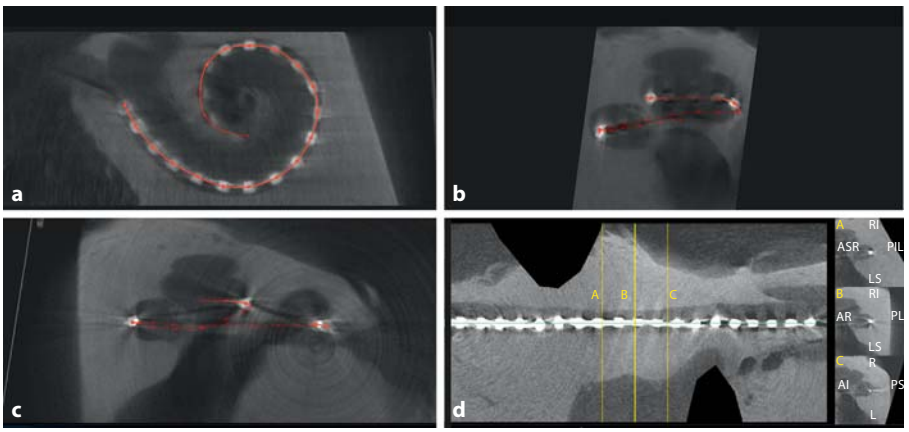

Fig. 8. CT scan of low-trauma insertion. A micro-CT scan was performed to evaluate the array position in the scala tympani in 3 orthogonal planes (**a–c**) and with a curved reconstruction along the array (**d**). In 4 of the 6 cases, the array was fully inserted and positioned in the inferior part of the cochlear lumen corresponding to the scala tympani. Representative example of a fully inserted array.

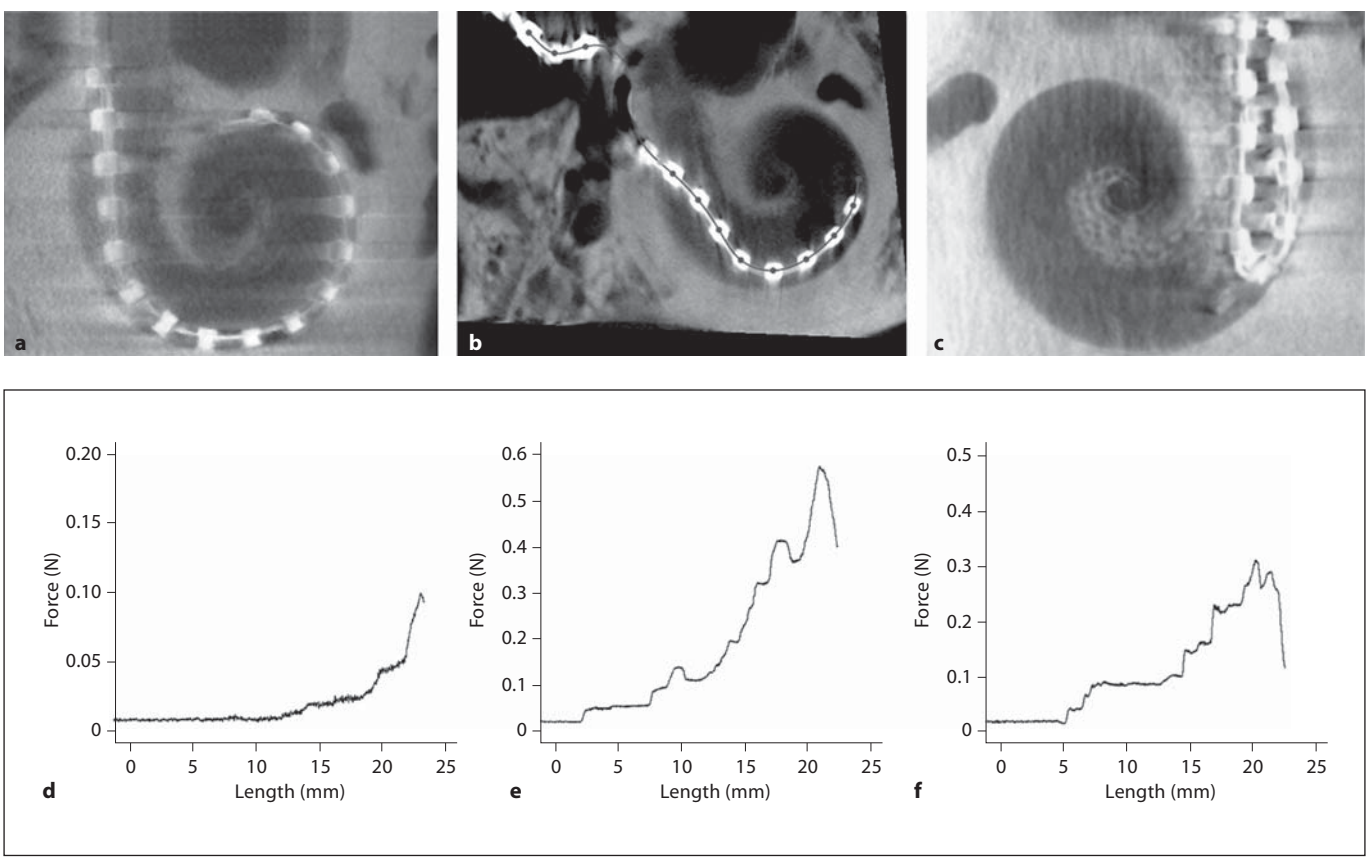

Fig. 9. Insertion force recordings and CT scans of traumatic insertions. A different force profile was observed in fully inserted arrays (**a**), in partially inserted arrays (**b**), and in a case of folding array tip (**c**). The fully inserted array had a low force profile with a peak force at 0.1 N and a slope rise after 20 mm (**d**). The partially inserted array had a peak force >0.5 N with a slope increase after 10 mm (**e**). The array with a folding tip had a peak force >0.3 N and a slope rise after only 7 mm (**f**).

translocation to the scala vestibuli or a fracture of the osseous spiral lamina represent critical damage that is probably related to high insertion forces. The relation between insertion forces and array progression can only be studied with synchronous force measurements and array visualization. Array progression inside a cochlea can be followed by fluoroscopy [Huttenbrink et al., 2002], but with this technique the basilar membrane perforation is hardly detected.

The major advantage of our model is the combination of real tissue friction conditions and the possibility to visualize the array progression in the scala tympani through the basilar membrane by transparency. Furthermore, the use of fresh temporal bones provides endosteum lining properties which are closer to those of a live tissue than formalin-fixed temporal bones. Finally, the 3D force sensor used in our model provided information on the x- and y-axis which cannot be obtained by a load beam cell used in the above-cited models.

A high rate of basilar membrane perforation was observed in both array types in this study (50% in the standard group, 40% in the prototype group) compared to previous reported series in the microdissected cochleae. For instance, Wardrop et al. [2005a, b] reported lower basilar membrane perforation in 2 series of arrays inserted manually: 8/26 and 7/28 basilar membrane perforation. This difference can be explained by the fact that our microdissected model has the drawback of potentially creating histological damage or a weakening of the basilar membrane before array insertion. Thus, spiral ligament or basilar membrane trauma during array insertion is probably overestimated in this model. Moreover, there was no real-time correction of the insertion axis once the insertion tool was started. We decided to stop the insertion only if the array buckled at the cochleostomy because it led to the exponential and irregular rise of force measurement. We also stopped data acquisition after a basilar membrane perforation because the array progression continued in an open scala vestibuli or outside the cochlea without any resistance. On the contrary, in intact cochlea models, force measurements can be pursued even if the array is translocated in the scala vestibuli.

In our study, we decided to use the temporal bone and the array only once. This study design was motivated by the assumption that once a cochlea has been implanted, a lower resistance path can be created as the first insertion might have damaged the inner ear structures. The disadvantage of this design is that the variability of cochlear size and shape might require a higher number of temporal bone specimens to achieve statistical significance.

Application to Array Design Comparison

In this study, we compared the depth of array insertion without stop, the basilar membrane perforation, and the insertion forces between standard and prototype arrays. The array designs differed by their proximal diameters (higher in the standard) and the presence of a distal tapering in the standard array. The comparison of insertion forces as a function of angle progression showed that the prototype array had lower friction forces beyond 270° compared to the standard array. This might be explained by a lower prototype array stiffness with lower radial force on the lateral wall and the array section surface/lumen ratio which is lower in the prototype, allowing it to progress further in the apex.

Considering the limitations of our model, the histological study and basilar membrane trauma cannot be used to compare arrays. The applied force necessary to perforate the basilar membrane is between 0.026 N in the apical turn and 0.035 N at the basal turn using a 130-μm-diameter cylinder needle applied perpendicularly to the basilar membrane [Ishii et al., 1995]. A thin array on the whole length should provide lower insertion forces and less risk to inner structures. In contrast, a larger array with a sharper tip, such as the standard array, should provide higher insertion forces concentrated on the sharp tip acting as a needle and possibly providing more basilar membrane perforation.

The array with a folding tip and the partially inserted array had different force profiles compared to the remaining fully inserted arrays. The peak force was higher and, more interestingly, the rising segment of the insertion force appeared earlier during the insertion. It is easily possible to automatically stop the insertion once this rising segment is detected. Thus, real-time force measurement and display during array insertion may enhance the quality of the insertion. It would also have been interesting to observe or predict the basilar membrane perforation on force profiles. However, it was impossible to detect such an event with our force sensor. A force sensor with much higher accuracy or placed at the tip of the array might be able to address this issue.

Conclusion

We describe a microdissected model of human cochlea implanted with a motorized tool to evaluate insertion forces during cochlear implantation. This model allowed real-time visualization of array progression in the human scala tympani under microscope. With this tech-

nique, we observed that the critical region for the basilar membrane damage is at 180° in the cochlea. The comparison of a standard (Digisonic SP) to a thinner prototype array showed lower forces and deeper insertions with the prototype array.

Acknowledgements

This work was partially funded by Neurelec Ltd. (Vallauris, France), Gueules Cassées Foundation (grant No. 25-2010), and Fondation de l'Avenir (grant ETO 568).

References

Adunka O, Kiefer J: Impact of electrode insertion depth on intracochlear trauma. Otolaryngol Head Neck Surg 2006;135:374–382.

Blamey P, Arndt P, Bergeron F, Bredberg G, Brimacombe J, Facer G, Larky J, Lindstrom B, Nedzelski J, Peterson A, Shipp D, Staller S, Whitford L: Factors affecting auditory performance of postlinguistically deaf adults using cochlear implants. Audiol Neurootol 1996;1:293–306.

Clark GM: Electrical stimulation of the auditory nerve: the coding of frequency, the perception of pitch and the development of cochlear implant speech processing strategies for profoundly deaf people. Clin Exp Pharmacol Physiol 1996;23:766–776.

Eshraghi AA, Yang NW, Balkany TJ: Comparative study of cochlear damage with three perimodiolar electrode designs. Laryngoscope 2003;113:415–419.

Gomaa NA, Rubinstein JT, Lowder MW, Tyler RS, Gantz BJ: Residual speech perception and cochlear implant performance in postlingually deafened adults. Ear Hear 2003;24:539–544.

Huttenbrink KB, Zahnert T, Jolly C, Hofmann G: Movements of cochlear implant electrodes inside the cochlea during insertion: an x-ray microscopy study. Otol Neurotol 2002;23:187–191.

Ishii T, Takayama M, Takahashi Y: Mechanical properties of human round window, basilar and Reissner's membranes. Acta Otolaryngol Suppl 1995;519:78–82.

Kiefer J, Gstoettner W, Baumgartner W, Pok SM, Tillein J, Ye Q, von Ilberg C: Conservation of low-frequency hearing in cochlear implantation. Acta Otolaryngol 2004;124:272–280.

Lazard DS, Bordure P, Lina-Granade G, Magnan J, Meller R, Meyer B, Radafy E, Roux PE, Gnansia D, Pean V, Truy E: Speech perception performance for 100 post-lingually deaf adults fitted with neurelec cochlear implants: comparison between digisonic(r) convex and digisonic(r) sp devices after a 1-year follow-up. Acta Otolaryngol 2010;130:1267–1273.

Lehnhardt E: Intracochlear placement of cochlear implant electrodes in soft surgery technique (in German). HNO 1993;41:356–359.

Majdani O, Schurzig D, Hussong A, Rau T, Wittkopf J, Lenarz T, Labadie RF: Force measurement of insertion of cochlear implant electrode arrays in vitro: comparison of surgeon to automated insertion tool. Acta Otolaryngol 2010;130:31–36.

Radeloff A, Unkelbach MH, Mack MG, Settevendemie C, Helbig S, Mueller J, Hagen R, Mlynski R: A coated electrode carrier for cochlear implantation reduces insertion forces. Laryngoscope 2009;119:959–963.

Roland JT Jr: A model for cochlear implant electrode insertion and force evaluation: results with a new electrode design and insertion technique. Laryngoscope 2005;115:1325–1339.

Wardrop P, Whinney D, Rebscher SJ, Luxford W, Leake P: A temporal bone study of insertion trauma and intracochlear position of cochlear implant electrodes. II. Comparison of spiral clarion and hifocus ii electrodes. Hear Res 2005a;203:68–79.

Wardrop P, Whinney D, Rebscher SJ, Roland JT Jr, Luxford W, Leake PA: A temporal bone study of insertion trauma and intracochlear position of cochlear implant electrodes. I. Comparison of nucleus banded and nucleus contour electrodes. Hear Res 2005b;203:54–67.

Wilson BS, Dorman MF: Cochlear implants: a remarkable past and a brilliant future. Hear Res 2008;242:3–21.